STUDY ON THE OPERATING EFFECT OF STRAW CRUSHING AND SPREADING DEVICES ON SINGLE AXIAL FLOW HARVESTERS

/

单纵轴流收获机装配秸秆粉碎抛撒装置作业效果问题研究

Jiang WANG[1)], **Longjing LI**[1)], **Weiliang SHI**[1)], **Youqiang DING**[2)*]
[1)] College of Automotive Engineering, Zibo Vocational Institute, Zibo/China;
[2)]Nanjing Institute of Agricultural Mechanization, Ministry of Agriculture and Rural Affairs, Nanjing/China
Tel: 18801239355; E-mail: dyq_cau@163.com
DOI: https://doi.org/10.35633/inmateh-75-41

Keywords: *Single Axial Flow; Harvesters; Straw Crushing; Straw Spreading; operating effect*

ABSTRACT

To identify the specific manifestations and influencing factors of the poor straw crushing and spreading effects in Northeast rice-growing areas, this paper focuses on the straw crushing and spreading device widely used on single axial flow harvesters. Experimental and theoretical analyses were conducted. The results indicate that the existing straw crushing and spreading devices, under different operating speeds and with various active blade types, exhibit crushing performance, spreading width, and spreading uniformity significantly below standard values. The primary issues are straw clumping, insufficient straw crushing, lateral bias in spreading, and inadequate spreading width. By establishing a theoretical model, the analysis reveals that the straw crushing effect is related to the characteristics of the straw itself, such as blade rotational speed, cutting angle, and support angle. In contrast, the spreading effect is associated with the motion direction of the straw leaving the threshing drum, straw ejection speed, and the arrangement of deflector plates. This paper clarifies the elements that need improvement in the operational effectiveness of the straw crushing and spreading devices attached to combine harvesters, providing a theoretical basis for subsequent enhancements.

摘要

为找到东北稻区秸秆粉碎抛撒效果差的具体表现形式及其影响因素，本文以广泛使用的单纵轴流收获机装配的秸秆粉碎抛撒装置为研究对象，开展试验和理论分析研究。试验表明，现有秸秆粉碎抛撒装置在不同作业速度下，采用不同动刀类型，粉碎抛撒装置粉碎效果、抛撒幅宽和抛撒不均匀度都远低于标准值，作业效果问题主要变现为：秸秆成团、秸秆粉碎不充分、抛撒偏向一侧、抛撒幅宽不足。通过建立理论模型分析得出，秸秆粉碎效果与秸秆自身特性，粉碎刀转速、开刃角、支撑角有关；抛撒效果与秸秆离开脱粒滚筒时运动方向、秸秆抛离速度、导流板布置有关。文章明确了联合收获机装配的秸秆粉碎抛撒装置作业效果需要提升的要素，为后续的改进提供理论依据。

INTRODUCTION

With the large-scale and intensive development of agriculture in China, single axial flow combine harvesters have become the mainstream products in the market due to their high efficiency and cost performance. These machines are particularly suitable for harvesting crops like rice (*Gong et al., 2024; Zhang et al., 2021*), which produce a substantial amount of straw and have gained significant usage in Northeast China (*Wang et al., 2021*). Returning straw to the fields can improve soil fertility, enhance soil structure, and increase grain yield (*Wang et al., 2023; Zang et al., 2021*), making it a critical measure for sustainable soil development (*Wang et al., 2017*). As a result, there is a growing demand for equipping combine harvesters with straw-crushing and spreading devices (*Wang et al., 2022*). However, in Northeast China's rice-growing areas, the ample and tough straw presents challenges, leading to poor crushing and spreading effects and unsatisfactory straw return quality (*Sun et al., 2019*).

Existing research on straw crushing and spreading (*Jankauskas et al., 2023; Li et al., 2023; Sun et al., 2019; Vlăduț et al., 2023; Vlăduț et al., 2023; Wang et al., 2021; Wang., 2018; Wang., 2018)* mainly focus on the design of the devices or the analysis of the product's application effects. There is a lack of detailed analysis of the causes of poor straw-crushing and spreading effects in this region.

More theoretical models must be developed to address these processes for the straw-crushing and spreading devices mounted on combine harvesters. This study conducts field experiments and theoretical analyses based on the original straw crushing and spreading devices of single axial flow combine harvesters. It aims to identify the specific problems and underlying causes in each stage of grinding and spreading while clarifying the aspects that need improvement, thus providing a foundation for future enhancements.

MATERIAL AND METHODS

Structure and Working Principle of the Straw Crushing and Spreading Device on Single Axial Flow Harvesters

The structure and spatial layout of the straw-crushing device mounted on this type of combine harvester are roughly illustrated in Fig.1. During operation, the straw crushing and spreading process can be divided into three stages:

(1) Straw Feeding Stage: Straw exits through the discharge opening of the threshing mechanism and slides down the collecting board to the entrance of the crushing device chamber.

(2) Straw Crushing Stage: After the straw enters the crushing device chamber, it is chopped up with the cooperation of the moving and fixed blades.

(3) Straw Spreading Stage: The crushed straw falls to the ground under the influence of the spreading device and its gravity.

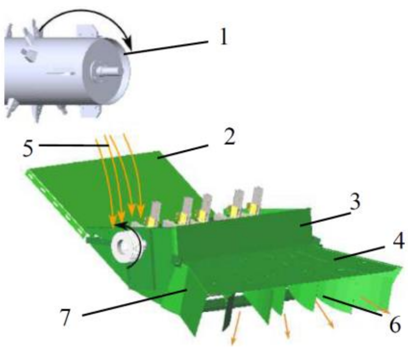

Fig. 1 - Schematic diagram of the spatial position of the single vertical axis flow harvester's straw crushing and spreading device

1. Threshing Mechanism; 2. Collecting Board; 3. Crushing Device; 4. Spreading Device; 5. Rice Straw; 6. Spreader Deflector Plate; 7. Spreader Housing

Experimental Design

Field experiments were conducted during the rice harvesting period using the John Deere C100 single vertical axis flow combine harvester to explore the factors affecting the performance of rice straw crushing and spreading operations, as shown in Fig.2. The stubble height was approximately 30 cm during the operation, as illustrated in Fig.3. The experiment was carried out at Experimental Field No. 36 in the Jian Sanjiang Farm of Heilongjiang Province, with the rice variety being Longjing 31. The average plant height was 94.62 cm, and the average panicle length was 15.94 cm, while the straw moisture content measured 33.01%.

Fig. 2 - John Deere C100 and Stubble height

Fig. 3 - Smooth blade and serrated blade

Fig. 4 - Field test image

The harvester's original straw crushing and spreading device uses a high-speed rotating swing knife and a single-row fixed knife. Both the fixed and moving knives have smooth blades (no serrations). The rotational speed of the knife shaft is 2600 r/min. The test compares the shredding and spreading effects of the moving knives, which are smooth-blade knives and serrated blades. As shown in Fig.3, the test-crushing moving knives use the original smooth blade and the serrated blade available on the market. After the smooth blade knife operation was completed, the knife shaft with the serrated knife was installed to replace the smooth blade knife shaft, and the test operation continued. The header width of the harvester was 4.5 m, and the feeding rate was 9 kg/s.

The test speed is based on the gear position of the harvester, and the first gear's low speed, the first gear's high speed, the second gear's low speed, and the second gear's high speed are selected. The corresponding speeds measured by the stopwatch are 0.95 m/s, 1.12 m/s, 1.21 m/s and 1.38 m/s.

The test used straw crushing qualified rate (crushing length <15 cm) y_1, straw spreading width (harvesting width 4.5 m) d, and spreading unevenness F_b as evaluation indicators. Fig.4 is a field test image.

The straw spreading width measurement method is: 5 measuring points are taken at equal intervals within the harvesting stroke of the combine harvester, and the width is measured and recorded at each measuring point. The straw sampling method is: one point is taken within the two working strokes of the combine harvester, and 5 sampling frames with an area of 90 cm × 50 cm are placed in sequence at each measuring point parallel to the direction of the harvester header, and all the straw in the sampling frame is collected. The straw crushing qualified rate and spreading unevenness are calculated according to the requirements of GB/T 24675.6-2009 "Conservation Tillage Machinery Straw Crushers (*GB/T 24675.6-2009-2009*). The calculation formulas for straw crushing qualified rate y_1 and spreading unevenness F_b are respectively:

$$y_1 = \frac{M_{ai} - M_{bi}}{M_{ai}} \times 100\%, \quad i = 1, 2....10 \tag{1}$$

$$F_b = \frac{1}{\overline{M}} \sqrt{\frac{1}{9} \sum_{i=1}^{10} (M_{ai} - \overline{M})^2} \times 100\%, \quad i = 1, 2....10 \tag{2}$$

where M_{ai} is the total mass of the straw at the sampling point, g; M_{bi} is the mass of the straw with a length less than 15 cm at the sampling point, g; and $\overline{M}$ is the average mass of the straw at each measuring point, g.

RESULTS

Test results and analysis

Fig.5 shows the changes in various test indicators with harvesting speed. Referring to the straw crushing qualification rate requirements in GB/T 24675.6-2009, it can be seen from Fig.5a that the operating results of different types of crushing knives are not ideal when crushing rice straw in Northeast China, all are far less than 85%, and the lowest operating speed is 0.95 m/s, the qualified rate of straw crushing with different crushing knife types is only 72.02% and 63.48%. At the same time, as the operating speed increases, the qualified rate of straw crushing also has a downward trend. Under the same operating conditions, the smooth-edged crushing knife has a higher straw crushing qualification rate than the serrated knife. Through actual observation of the shape of the straw after different knife types, it was found that the straw incision showed more tearing after being crushed by the serrated knife. Fig.5b reflects that the change of the blade of the movable knife has no significant impact on the throwing width. It is observed that the straw throwing width of the modified machine is significantly different from the harvesting width, and as the operating speed increases, the throwing width decreases. Fig.5c shows that the throwing unevenness of both knife types is poor, which is far from the standard requirement of less than 30%. As the speed increases, the throwing unevenness slightly increases. According to the test, the operating effect of this model's straw crushing and spreading device could be better, and it needs to continue to be improved to solve the critical technical problem of straw crushing and spreading that restricts the quality of straw return to the field.

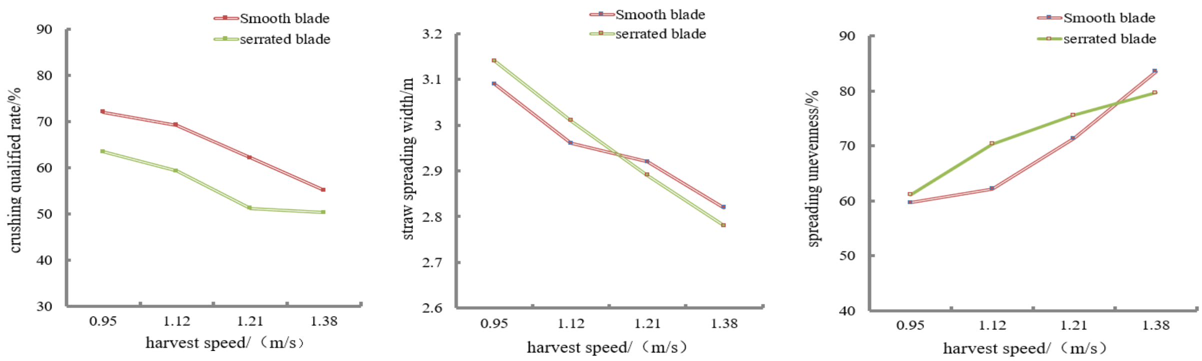

(a) Crushing qualification rate (b) Spreading width (c) Spreading unevenness

Fig. 5 - Variation of each test index with harvesting speed

Existing problems and theoretical analysis

Study on crushing problems

The straw scattered on the ground after the observation test is shown in Fig.6. After the observation operation, the straw mainly clumped together. As shown in Fig.6a, many straws were over 20 cm long, which severely impacted the subsequent straw burial and field return effectiveness (*Sun et al., 2019*). It was also found that the straw length did not meet the standard due to insufficient crushing. The straw shape exhibited one or more bends and damages along the straw shaft, as shown in Fig.6b. The main reason for this damage was that the moving and fixed knives failed to cut effectively into the straw. The excessive straw length also contributed to clumping.

(a) Clumping after operation (b) Insufficient shredding of straw

Fig. 6 - Straw scattered on the ground

(1) Analysis of straw cutting force

As an elastic body, straw undergoes two distinct stages during cutting: (1) the initial contact of the moving blade with the straw, leading to extrusion deformation, and (2) the continued movement of the moving blade, causing the straw to plastically deform before being cut. Effective straw cutting occurs in the second stage, making it crucial to study the force state of the moving blade during this phase. Establishing a mechanical model will aid in analyzing the key factors that influence the cutting effect in greater depth.

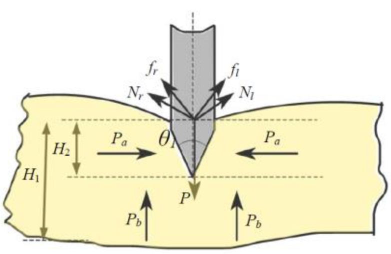

Fig. 7 - Model diagram of a moving knife cutting into a single straw

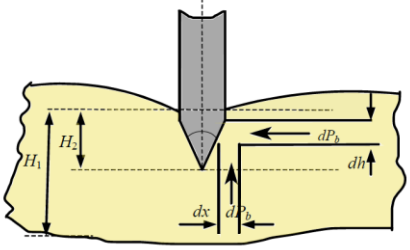

Fig. 8 - Schematic diagram of horizontal and vertical differential forces

As shown in Fig.7, a vertical cross-section model is established when the moving knife cuts into a single straw and the blade is sharpened on both sides. The force applied to the blade during the cutting process is analyzed. During the cutting process, the blade will be subjected to the extrusion force N_l and N_2 of the straw stem on the blade, which is perpendicular to the sharpening surface in the opposite direction. Under the action of the extrusion force, friction forces f_l and f_2 will be generated simultaneously. Because the sharpening is symmetrical, ignoring the differences in the microstructure inside the stalk, it can be assumed that N_l=N_2 and f_l=f_2. Therefore, it can be seen that the cutting force P on the straw at the moment the blade cuts in can be expressed as:

$$\begin{cases} P = 2(N_1 \sin\dfrac{\theta_1}{2} + f_1 \cos\dfrac{\theta_1}{2}) \\ f_1 = \mu N_1 \end{cases} \tag{3}$$

where θ_1 is the blade angle of the moving blade, °; μ is the friction coefficient of rice straw.

During the extrusion deformation process of the moving blade, the extrusion force N_l acting on the grinding blade surface can be decomposed into the horizontal extrusion force P_a and the vertical extrusion force P_b of the straw on the blade (*Koolen,1994*), so:

$$N_1 = P_a \sin\frac{\theta_1}{2} + P_b \cos\frac{\theta_1}{2} \tag{4}$$

To bring in factors related to straw characteristics, the extrusion pressure P_a and pressure P_b in the above formula can be obtained by integrating the differential forces in their respective directions (*Zhao et al., 2015*), as shown in Fig.8. As an elastic body, according to Hooke's law, the strain of straw after impact ε can be expressed as:

$$\varepsilon = \frac{\sigma}{E} = \frac{h_x}{H_1} \tag{5}$$

where σ is the stress when the straw is cut, N; E is the instantaneous elastic modulus of the straw when the knife cuts the straw; H_1 is the diameter of the straw before it is cut, mm; h_x is the thickness of the straw after it is squeezed, mm.

Therefore, the vertical squeezing force dP_b acting on the unit length of the straw can be expressed as:

$$dP_b = E\varepsilon \tan\frac{\theta_1}{2} dh_x \tag{6}$$

By integrating both ends of the above equation, the vertical extrusion force P_b can be obtained:

$$P_b = \frac{E}{H_1}\tan\frac{\theta_1}{2}\int_0^{H_2} h_x dh_x = \frac{E}{2H_1}H_2^2 \tan\frac{\theta_1}{2} \tag{7}$$

where H_2 is the thickness of the straw when it is plastically deformed by extrusion, mm.

Similarly, the horizontal extrusion force P_a can be obtained:

$$P_a = \frac{\nu E}{H_1}\int_0^{H_2} h_x dh_x = \frac{\nu E}{2H_1}H_2^2 \tag{8}$$

where ν is the Poisson's ratio of the straw.

Substituting equations 4, 7, and 8 into equations 3, the instantaneous cutting force P on the straw is obtained:

$$P = \frac{EH_2^2}{H_1}\left[\nu(\sin^2\frac{\theta_1}{2} + \mu\sin\frac{\theta_1}{2}\cos\frac{\theta_1}{2}) + \tan\frac{\theta_1}{2}(\sin\frac{\theta_1}{2}\cos\frac{\theta_1}{2} + \mu\cos^2\frac{\theta_1}{2})\right] \tag{9}$$

When the instantaneous impact on the straw is more significant, the possibility of the knife cutting into the straw will be greater. According to Equation 9, the instantaneous cutting force on the straw is related to the characteristics of the straw itself. The friction coefficient of the straw and the resistance to bending of the straw impact the instantaneous force. The cutting angle of the moving knife also positively impacts the instantaneous force on the straw, so the cutting angle can be reasonably optimized when designing the blade. In addition, according to Formula 9, it can also be found that when the instantaneous extrusion thickness H_2 of the straw increases, the instantaneous cutting force of the straw increases significantly. Changes in the extrusion thickness H_2 are often related to the movable knife's rotational speed and the cutting blade's support angle. However, due to the straw's stable characteristics, when the movable knife's rotational speed reaches a specific value, the instantaneous extrusion thickness of the straw will not change. When the movable fixed knife supports cutting, increasing the straw cutting support angle can effectively prevent the movement of the movable knife caused by the poor bending strength of the straw, thereby obtaining a greater extrusion thickness. Therefore, when the cutting knife rotates at a certain speed, the straw support characteristics of the crushing knife can improve the straw-cutting effect.

Study on the spreading problem

The harvesting operation test found that the original straw crushing and spreading device had a poor operation effect, and the uneven spreading degree was significantly different from the national standard requirements. Through experimental observation, the main manifestations were: the straw spreading was biased to one side (along the left side of the operation direction), and the straw spreading power was insufficient, resulting in a small spreading width. As shown in Fig.9, the single longitudinal axial flow combine harvester had the phenomenon of straw spreading biased to one side during the crushing and spreading operation. During the operation, no straw was thrown on the right side of the spreading device (in the red frame of the Fig.9), so the straw after throwing was mainly distributed on the left side of the harvester center line, resulting in uneven spreading. As shown in Fig.10, the harvesting width of the entire harvester is D, m; the width of the thrown straw distributed on the left side of the harvester center line is expressed as d, m; in the actual operation process, it was observed that $d<D/2$ and the difference was significant, so the spreading width was small and insufficient to match the harvesting width.

Fig. 9 - Spreading to one side

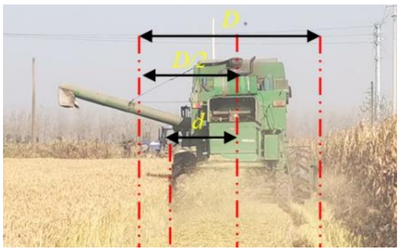

Fig. 10 - Spreading width is insufficient

Fig. 11 - Uneven straw feeding

(1) Study on the problem of spreading to one side

The movement of straw in the chamber of the crushing device is mostly tangential along the rotation of the crushing blade shaft (*Mu, 2021*). The spreading of straw to one side cannot be attributed to the axial movement of the straw during crushing. Instead, a possible cause is the uneven feeding of straw into the crushing device. To verify this hypothesis, the harvester crushing and spreading device was removed, and the straw flow state was observed after it left the threshing drum and before it entered the crushing device via the grass receiving plate. The straw flow direction is shown in Fig.11. It was observed that the straw flow was already biased to one side after leaving the drum and before entering the crushing device. The straw was not evenly distributed horizontally along the lower edge of the grass receiving plate, leading to the final uneven spreading of straw.

Considering that the straw crushing and spreading device equipped with the combine harvester operates on the straw discharged from the threshing device, the motion analysis of the state of the straw discharged from the threshing drum was carried out. Taking the straw flow with a specific volume as the research object, ignoring the entanglement, squeezing, and dragging effects caused by the continuous discharge between the straw flows, the surface velocity of the straw flow is decomposed. The *x*-axis direction is to the right in the width direction of the harvester; that is, the right direction is perpendicular to the forward direction of the harvester, and the *z*-axis direction is vertically upward. As shown in Fig.12, the straw flow will still maintain the tangential velocity v_1 rotating with the threshing drum and the movement velocity v_2 along the surface of the roller grass discharge board due to the centrifugal force of rotation and the support of the roller grass discharge board surface at the moment of separation. At the same time, the straw flow also accelerates a_0 due to its gravity at the moment of separation.

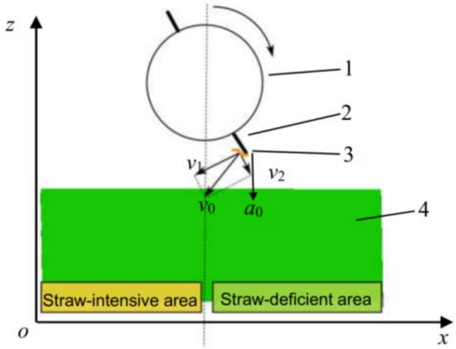

Fig. 12 - Kinematic analysis of the moment when the straw flow leaves the straw discharge plate

1.Threshing device; 2. Grass discharge board; 3. Straw flow; 4. Grass receiving board

Therefore, the instantaneous velocity v_0 of the straw flow leaving the roller straw discharge plate can be expressed as:

$$v_0 = \sqrt{v_1^2 + v_2^2} \tag{10}$$

In the formula, v_1 is the rotation speed of the threshing drum, m/s; v_2 is the movement speed of the straw along the surface of the drum discharge plate, m/s.

According to the literature (*Chen et al., 2020; Li et al., 2021*), it can be seen that the rotation speed of grain threshing equipment is generally 500~800 r/min, so the speed v_1 is larger than the speed v_2. Therefore, according to the speed synthesis parallelogram rule, the direction of the speed v_0 is closer to the speed v_1, which means that the discharged straw flow tends to move to the left.

Although there will be a vertical component force under the action of gravity during the period from when the straw flow breaks away from the straw discharge plate of the drum to when it starts to contact the crushing device and the straw plate, it will not significantly change the direction of the straw flow in a very short time. The continuous flow will form a dense area of straw on the left and a missing area of straw on the right at the bottom of the straw connecting plate of the crushing device. As shown in Fig. 12, this uneven straw feeding into the crushing device ultimately results in a deflected discharge, causing the crushed straw to be cast toward the left side.

From the above analysis, improving the uniformity of the transverse distribution of straw in the straw feeding and crushing device of a single longitudinal axis harvester is extremely important for reducing the unevenness of straw throwing. When optimizing the design, the direction of the straw falling off the drum can be guided, utilizing turbulence to counteract the tendency of the straw to move to the left. This approach helps ensure a more even distribution of straw when it is fed into the crushing device at the bottom of the straw plate.

(2) Research on the problem of insufficient throwing width

A dynamic model of the throwing width was established to study the factors influencing the throwing width of the straw crushing and throwing device assembled with the harvester. At the same time, it was assumed that the up and down rotation of the throwing device and the left and proper adjustment of the deflector did not affect the straw-throwing position. During the process of spreading straw in space, the right direction of the harvester width is used as the *x*-axis, the opposite direction of the working forward direction (i.e. backward) is used as the *y*-axis, and the vertical direction is used as the *z*-axis to establish a coordinate system and scatter the straw in the three-dimensional space. The motion is decomposed into *yoz* and *xoy* plane motions, as shown in Fig.13. v_c represents the operating direction and speed of the harvester, m/s; H_p is the height of the straw throwing point from the ground, m; w_c is the distance between the outermost deflector and the center line of the throwing device, m; w_b is the straw throw distance from the deflector. The movement distance along the *x*-axis after exiting, m; w_p is half of the width of the straw throwing width, m. The straw throwing speed is v_b, and the corresponding speeds decomposed into the *x*, y, and *z* axes are v_{b1}, v_{b2}, and v_{b3}.

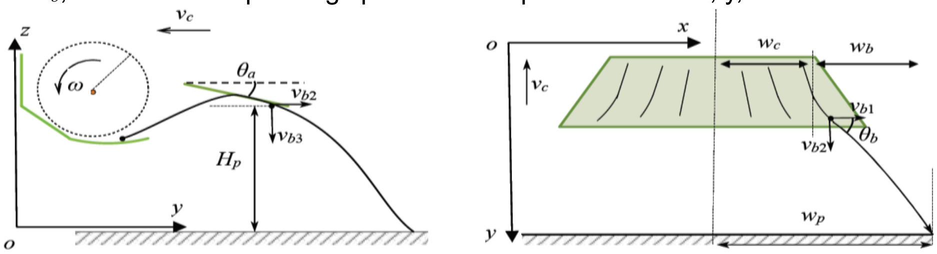

(a) Straw spreading *yoz* plane (b) Straw spreading *xoy* plane

Fig.13 - Straw spreading trajectory of the straw crushing and spreading device

According to Fig.13b, the straw spreading width is twice w_p, and w_p can be expressed as:

$$w_p = w_c + w_b \tag{11}$$

From formula 11, it can be seen that the farthest distance determines the size of the straw spreading width. The straw is thrown under the guidance of the outermost guide plate. When the height H_p of the straw spreading point from the ground remains constant, the velocity v_{b1} of v_b along the *x*-axis determines the movement distance of the straw along the *x*-axis. The straw spreading motion can be analyzed using the theory of projectile motion. Referring to relevant literature *(Brown, 2001)*, the motion equation of the straw along the x-axis during the spreading process is:

$$\begin{cases} \dfrac{d^2x}{dt^2} + k_a \left(\dfrac{dx}{dt}\right)^2 = 0 \\ k_a = \dfrac{\rho_a c_a A_a}{2m'} \end{cases} \tag{12}$$

where k_a is the air resistance factor; m' is the mass of the straw to be scattered, kg; ρ_a is the air density, kg/m^3; c_a is the air damping coefficient; A_a is the resistance area caused by the shape and size of the straw, m^2.

To obtain the speed of the straw along the x-axis during the spreading process, equation 12 is integrated and solved. Assume that the initial conditions for spreading are: at spreading time t=0, $v_{bx}(0)=v_{b1}$, $x(0)=w_c$, and the speed of the straw along the *x*-axis at time *t* is solved as follows:

$$v_{bx}(t)=\frac{dx}{dt}=\frac{v_{b1}}{1+k_a v_{b1} t} \tag{13}$$

The position coordinates of the straw along the *x*-axis during the spreading process can be expressed as:

$$x(t)=w_c+\int_0^t v_{dx}(t)dt=w_c+\frac{1}{k_a}\ln(1+k_a v_{b1} t) \tag{14}$$

wherein, according to the spatial geometric relationship, the velocity v_{b1} along the *x*-axis can be expressed by the initial velocity of the straw spreading:

$$v_{b1}=\frac{\cot\theta_b}{\sqrt{1+\tan^2\theta_a+\cot^2\theta_b}}v_b \tag{15}$$

Substituting equation 15 into equation 14, it can be obtained:

$$x(t)=w_c+\frac{1}{k_a}\ln(1+\frac{k_a\cot\theta_b}{\sqrt{1+\tan^2\theta_a+\cot^2\theta_b}}v_b t) \tag{16}$$

where θ_a is the installation angle of the spreading device, °; θ_b is the angle between the straw throwing speed and the *x*-axis, °.

Assuming that the time for the straw to fall to the ground after spreading is t_1, the value of w_c can be obtained by substituting it into the above formula. When the installation position of the spreading device is fixed, the installation angle is no longer adjusted, and external conditions remain constant due to the limited landing height, it can be considered that the straw landing time t and the air resistance factor k_a are fixed values. Under these conditions, the straw spreading distance w_p is only related to the throwing speed v_b and the angle θ_b between the throwing speed v_b and the *x*-axis. The magnitude of the straw throwing speed v_b is influenced by the airflow speed generated during the straw crushing process. The crushed straw will produce collisions and friction under the drainage action of the guide plate. This process can also increase the straw-throwing speed by reducing the kinetic energy loss. Therefore, a well-optimized guide plate layout angle can further enhance the spreading width.

CONCLUSIONS

Through an in-depth analysis of the problems existing in the operation of the original crushing and spreading device of the single longitudinal axial flow combine harvester, the factors requiring improvement in the straw feeding, crushing, and spreading stages were determined. The main conclusions of this study are as follows:

1. Through field test research, it was found that the problems existing in the operation of the straw crushing and spreading device equipped with the combine harvester in the rice-growing area of Northeast China were mainly manifested as straw clumping, insufficient straw crushing, spreading to one side, and insufficient spreading width.

2. A straw-crushing dynamics model was established, and the analysis revealed that the straw-crushing effect is influenced by the characteristics of the straw itself, the crushing knife speed, the blade angle, and the support angle. When the cutting knife operates at a certain speed, enhancing the support characteristics of the crushing knife on the straw can significantly improve the straw-cutting effect.

3. The kinematic models of the straw leaving the threshing drum and the guide plate were established respectively. The analysis showed that the straw flow discharged from the drum tended to move to the left, resulting in uneven straw feeding into the crushing device, which ultimately caused the crushed straw to be thrown to the left. When the installation position of the throwing device was fixed and the installation angle remained unchanged, the throwing width was influenced by the straw throwing speed and the installation angle of the guide plate.

ACKNOWLEDGEMENT

This research was funded by Funded by Shandong Postdoctora1 Science Foundation (SDCX-ZG-202400013), National Key Research and Development Project （20106YFD0300909-3）.

REFERENCES

[1] Brown M.C. (2001). *Velocity Measurements Near an Automotive Cooling Fan*, Master Thesis, University of Windsor.

[2] Chen Y.P., Kang Y., Wang T.E., Ning X.J., Jin C.Q., Yin X. (2020). Distribution law of threshing material from longitudinal axial flow flexible threshing device of soybean harvester (大豆收获机纵轴流柔性脱粒装置脱出物分布规律). *Journal of China Agricultural University*, 25(09), pp. 104-111, DOI: 10.11841/j.issn.1007-4333.2020.09.11.

[3] GB/T 24675.6-2009-2009 Conservation tillage machinery Straw crusher and return machine (保护性耕作机械 秸秆粉碎还田机).

[4] Gong J.L., Luo Z.J., Zhang Y.F. (2024). Optimized design and simulation analysis of longitudinal flow corn cone threshing device. *INMATEH - Agricultural Engineering*, 73(2), pp.63-72, DOI: 10.35633/inmate-73-05.

[5] Jankauskas V., Abrutis R., Žunda A., Gargasas J. (2023). Wear Study of Straw Chopper Knives in Combine Harvesters. *Applied Sciences*, 13(13), 7384, pp 1-19, https://doi.org/10.3390/app13137384.

[6] Koolen A.J. (1994). Chapter 2 - Mechanics of Soil Compaction. *Developments in Agricultural Engineering,* 11, pp 23-44, DOI: 10.1016/B978 - 0 - 444 - 88286 - 8.50010 – 6.

[7] Li H.B., Wang Q.H., Ma J., Yue D., Geng D. (2023). Design and experiment of transverse axial flow corn flexible threshing device. *INMATEH - Agricultural Engineering*, 69(1), pp. 461-470, DOI: https://doi.org/10.35633/inmateh-69-43.

[8] Li X.P., Wang W.Z., Zhao G.Y., Sun C.C., Hu P.Z., Ji J.T. (2021). Design and Experiment of Rice Straw Chopping Device for Agitation Sliding Cutting and Tearing (纵轴流双柔性碾搓式谷子脱粒装置设计与试验). *Transactions of the Chinese Society of Agricultural Machinery*, 52(07), pp. 113-123, DOI: 10.6041/j.issn.1000-1298.2021.07.011.

[9] Mu G.Z. (2021). *Study on Key Technologies and Devices of Crushing and Throwing in Ridge-Imitating Sweet Potato Vine Recycling Machine (仿垄式甘薯秧回收机粉碎抛送关键技术与装置研究)*, PhD dissertation, Shandong Agricultural University.

[10] Sun N.N., Wang X.Y., Li. H.W., He J., Wang Q., Wang J., Liu Z., Wang Y. (2019). Design and experiment of differential sawing rice straw chopper for turning to field (差速锯切式水稻秸秆粉碎还田机设计与试验), *Transactions of the Chinese Society of Agricultural Engineering*, 35(22), pp. 367-276, DOI: 10.11975/j.issn.1002-6819.2019.22.032.

[11] Vlăduț V., Biris S.Ș., Paraschiv G., Ungureanu N., Bungescu S.T., Voiceal I., Cujbescu D., Găgeanu I., Laza E., Popa L.D., Matel G., Atanasov A. (2023). Considerations regarding the effects of shocks and vibrations on operators of self-propelled agricultural equipment. *INMATEH - Agricultural Engineering*, 52(07), pp. 843–856, https://doi.org/10.35633/inmateh-71-74.

[12] Vlăduț N.V., Ungureanu N., Biriș S.Ș., Voicea I., Nenciu F., Găgeanu I., Cujbescu D., Popa L.D., Boruz S., Matei G., Ekielski A., Teliban G.C. (2023). Research on the Identification of Some Optimal Threshing and Separation Regimes in the Axial Flow Apparatus. *Agriculture*, 13(4), 838, pp.1-17, https://doi.org/10.3390/agriculture13040838.

[13] Wang J., Wang X.Y., Li. H.W., He J., Lu C., Liu D. (2021). Design and experiment of rice straw chopping device for agitation sliding cutting and tearing (水稻秸秆激荡滑切与撕裂两级切割粉碎装置设计与试验), *Transactions of the Chinese Society of Agricultural Machinery*, 52(10), pp. 28-40, https://nyjxxb.net/index.php/journal/article/view/1243.

[14] Wang J., Wang X.Y., Li. H.W., Lu C.Y., He j., Wang Q.J., Liu D., Deng B., Zhang M.Y. (2022). Improvement of Straw Throwing Performance of Harvester Based on Matching Header Width. *Agriculture*, 12(9), 1291 pp. 1-20, https://doi.org/10.3390/agriculture12091291.

[15] Wang J.W., Tang H., Wang J.F. (2017). Comprehensive Utilization Status and Development Analysis of Crop Straw Resource in Northeast China (东北地区作物秸秆资源综合利用现状与发展分析). *Transactions of the Chinese Society of Agricultural Machinery*, 48(05), pp. 1-21, DOI:10.6041/j.issn.1000-1298.2017.05.001.

[16] Wang X. (2018). *Design and Test of Shredding and Scattering Machine for Longitudinal Axial Flow Rice and Wheat Combine Harvester (纵轴流稻麦联合收获机后切碎抛撒装置设计与试验)*, Master Thesis, Chinese Academy of Agricultural Sciences.

[17] Wang X., Jin C.Q., Xu J.S., Ni Y.L. (2018). Research status and trend of the crop straws of combine harvester (联合收割机后秸秆切碎抛撒研究现状与趋势). *Journal of Chinese Agricultural Mechanization*, 39(01), pp. 1-6, DOI：10.13733/j.jcam.issn.2095-5553.2018.01.001.

[18] Wang Z.T., Ling J., Liu Z.X., Zhao D.Q., Li Z.X., Zhou S.L., Yuan X.M., Li X.H., Wen Y. (2023). Effect of straw return practices on soil physico-chemical properties and maize yield (秸秆还田方式对土壤理化性质和玉米产量的影响), *Chinese Journal of Eco-Agriculture*, 32(04), pp. 663-674, DOI: 10.12357/cjea.20230517.

[19] Zhao F.Q., Wu C.Y., Huang M.S. (2015). Analysis of the cutting mechanism for straw chopper mounted on whole feeding combine harvester (全喂入联合收割机切碎装置茎秆切割机理分析). *Journal of Chinese Agricultural Mechanization*, 36(02), pp. 9-12, DOI: 10.13733/j.jcam.issn.2095-5553.2015.02.003.

[20] Zhang H, Hobbie E.A, Feng P., Zhou Z., Niu L., Duan W., Hao J., Hu K. (2021) Responses of soil organic carbon and crop yields to 33-year mineral fertilizer and straw additions under different tillage systems. *Soil and Tillage Research*, 209, 104943, pp. 1-9, https://doi.org/10.1016/j.still.2021.104943.

[21] Zhang Z.Z., Xie F.P., Tian L.Q., Liu D.W., Wang X.S., Li X. (2021). Current situation and development trend of threshing and separating system of international grain combine harvester (国外谷物联合收割机脱粒分离系统发展现状与展望). *Journal of Chinese Agricultural Mechanization*, 42(1), pp. 20-29, DOI: 10.13733/j.jcam.issn.2095-5553.2021.01.004.